Transfer reactions in 206Pb+118Sn: From quasielastic to deep-inelastic processes

Diklić, J.; Szilner, S.; Corradi, L.; Mijatović, T.; Pollarolo, G.; Čolović, P.; Colucci, G.; Fioretto, E.; Galtarossa, F.; Goasduff, A.; ...

Source / Izvornik: **Physical Review C, 2023, 107**

Journal article, Published version
Rad u časopisu, Objavljena verzija rada (izdavačev PDF)

https://doi.org/10.1103/PhysRevC.107.014619

Permanent link / Trajna poveznica: https://urn.nsk.hr/urn:nbn:hr:217:371045

Transfer reactions in ^{206}Pb + ^{118}Sn: From quasielastic to deep-inelastic processes

J. Diklić,[1] S. Szilner,[1,*] L. Corradi,[2,†] T. Mijatović,[1] G. Pollarolo,[3] P. Čolović,[1] G. Colucci,[4,5] E. Fioretto,[2] F. Galtarossa,[4] A. Goasduff,[2] A. Gottardo,[2] J. Grebosz,[6] A. Illana,[2,7] G. Jaworski,[5] M. Jurado Gomez,[8] T. Marchi,[2] D. Mengoni,[4] G. Montagnoli,[4] D. Nurkić,[9] M. Siciliano,[2,10] N. Soić,[1] A. M. Stefanini,[2] D. Testov,[4] J. J. Valiente-Dobón,[2] and N. Vukman[1]

[1]*Ruđer Bošković Institute, HR-10 001 Zagreb, Croatia*
[2]*Istituto Nazionale di Fisica Nucleare, Laboratori Nazionali di Legnaro, I-35020 Legnaro, Italy*
[3]*Dipartimento di Fisica, Università di Torino, and Istituto Nazionale di Fisica Nucleare, I-10125 Torino, Italy*
[4]*Dipartimento di Fisica e Astronomia, Università di Padova, and Istituto Nazionale di Fisica Nucleare, I-35131 Padova, Italy*
[5]*Heavy Ion Laboratory, University of Warsaw, PL-02093 Warsaw, Poland*
[6]*The Henryk Niewodniczanski Institute of Nuclear Physics, PL-31342 Krakow, Poland*
[7]*Accelerator Laboratory, Department of Physics, University of Jyväskylä, FI-40014 Jyväskylä, Finland*
[8]*Instituto de Física Corpuscular CSIC, E-46980 Valencia, Spain*
[9]*Physics Department, Faculty of Science, University of Zagreb, HR-10000 Zagreb, Croatia*
[10]*Physics Division, Argonne National Laboratory, Argonne, Illinois 60439, USA*

(Received 28 November 2022; accepted 24 January 2023; published 30 January 2023)

We measured multinucleon transfer reactions for the ^{206}Pb + ^{118}Sn system at $E_{lab} = 1200$ MeV by employing the large solid angle magnetic spectrometer PRISMA. Differential and total cross sections and Q-value distributions have been obtained for a variety of neutron and proton pick-up and stripping channels. The Q-value distributions show how the quasielastic and deep inelastic processes depend on the mass and charge of the transfer products. The corresponding cross sections have been compared with calculations performed with the GRAZING code. An overall good agreement is found for most of the few nucleon transfer channels. The underestimation of the data for channels involving a large number of transferred nucleons indicates that more complicated processes populate the given isotopes.

DOI: 10.1103/PhysRevC.107.014619

I. INTRODUCTION

Multinucleon transfer reactions between heavy ions at energies close to the Coulomb barrier constitute a link between quasielastic (QE) processes, characterized by the transfer of few nucleons and small kinetic-energy losses, and deep-inelastic (DIC) processes, where massive transfer and large kinetic-energy losses take place. In the QE regime nuclear structure plays a fundamental role in the evolution of the reaction and this is where specific properties, single particle degrees of freedom, surface vibrations, and pair transfer modes, can be probed at best [1,2]. Investigating how and up to what extent these properties govern the transition from the QE to DIC regimes has been the subject of very large amount of works over the last four decades, but the understanding of their details still faces significant experimental and theoretical challenges.

In recent years a renewed interest in the study of these processes has been motivated by advances in two main areas. On one side multinucleon transfer reactions have been recognized as a competitive and promising tool for the production of exotic species, especially the heavy neutron-rich ones which are accessible in reactions with very heavy systems [3]. On the other side it has been shown how nucleon-nucleon correlation properties can be quantitatively studied at energies far below the Coulomb barrier, where QE processes dominate [4,5]. These new studies are receiving a distinctive boost thanks to the successful implementation of large solid angle magnetic spectrometers, which allow to identify in mass, charge, and Q value and with unprecedented efficiency multinucleon transfer products. The experimental high-quality data accumulated so far on the relevant observables [6–14], in particular cross sections, also helped to test and improve the predictions of the various theoretical models [15–20]. However, such studies are still limited to very few cases and an effort is required to explore a wider range of bombarding energies and masses. This is particularly important for very heavy systems since they are notoriously affected by the high Coulomb field and by processes with large energy loss components, which may significantly influence the final yield distributions.

In this context we studied the ^{206}Pb + ^{118}Sn system at an energy high enough to get large mass and charge yields for multineutron and multiproton transfer channels, thus allowing to study in detail how the main observables, cross sections, and Q-value distributions, evolve as a function of the number of transferred nucleons. The specific choice of the isotopes has been done mainly because the optimum Q values are suitable for observing both neutron and proton pick-up and stripping

*Suzana.Szilner@irb.hr
†Lorenzo.Corradi@lnl.infn.it

channels (the terms pick-up and stripping are conventionally referred to the lighter partner of the reaction). Into more detail, the ground-to-ground state Q values for the main open channels lie below the bell-shaped curves which define the optimum Q values and therefore the transition probability [2]. These curves, a few MeV wide, are derived from the conditions of smooth matching of the entrance and exit channel trajectories [21]. In the presently studied system, of particular relevance are the channels associated with the neutron stripping and proton pick-up, since they lead to the population of heavy neutron-rich nuclei. This path, in heavy systems, has been studied in high-resolution experiments [11,12] using large solid-angle spectrometers. In the ^{136}Xe + ^{198}Pt reaction [11] it was evidenced that the production of very neutron-rich heavy nuclei was associated with low kinetic-energy losses. Besides the yields of the Xe-like fragments, those of the U-like nuclei were directly extracted via coincidences with γ rays in the ^{136}Xe + ^{238}U reaction [12]. Sizeable cross sections for neutron-stripping channels have been measured in the ^{94}Rb + ^{208}Pb reaction employing a neutron rich ^{94}Rb radioactive beam [22] and in the ^{197}Au + ^{130}Te reaction [14] employing a high-resolution kinematic-coincidence set-up. In this last system the effect of the neutron evaporation generated by large energy losses and its impact on the survival probability of the heavy Au isotopes was deduced. In the present study we investigated how, in heavy systems, the mass and charge yields and the final cross sections depend on the energy losses in their evolution from the QE to DIC regimes, testing up to what extent we can understand and describe on the same footing the whole set of neutron- and proton-transfer channels, opened along the pick-up and stripping directions.

II. THE EXPERIMENT

A ^{206}Pb beam was accelerated at $E_{\rm lab} = 1200$ MeV with an average current of ≈ 2 pnA employing the PIAVE positive-ion injector followed by the ALPI post-accelerator of Legnaro National Laboratories. A 200 μg/cm^2 strip (2 mm) ^{118}Sn target, with an isotopic purity of 99.6%, sandwiched between 15 μg/cm^2 carbon layers, was used. We detected target-like fragments in PRISMA [10], which was placed at $\theta_{\rm lab} = 35^\circ$ (the grazing angle) and, in an additional short run, at 25°, an angular range sufficiently wide to consistently follow the drop in yield of the elastic + inelastic scattering and the main region of the multinucleon transfers. Favorable experimental conditions were achieved by employing inverse kinematics, which allowed to get good A, Z, and Q-value resolution, thanks to the high kinetic energy (6–8 MeV/A) of the detected ions. Monitors of silicon surface barrier type were placed inside a sliding seal scattering chamber at $\theta_{\rm lab} = 50^\circ$–$65^\circ$. The monitors were used to detect Rutherford scattered Sn ions for relative normalization between different runs and to control the beam conditions during the measurements.

The identification of target-like products in PRISMA has been done on an event-by-event basis through the reconstruction of the trajectories of the ions [10] inside the magnetic elements. A start signal for time-of-flight measurements and two-dimensional position information are given by a position-sensitive microchannel plate detector [23]. After passing through a quadrupole and a dipole magnetic element, ions enter a focal plane made of a parallel-plate detector of multiwire type, providing timing and position signals, followed by an array of transverse-field multiparametric ionization chambers (IC) [24], where the nuclear charge Z is identified via energy-loss (ΔE) and total-energy (E) measurements. The magnetic fields of the spectrometer were set to bring the target-like ions with maximum yield near the center of the focal-plane area.

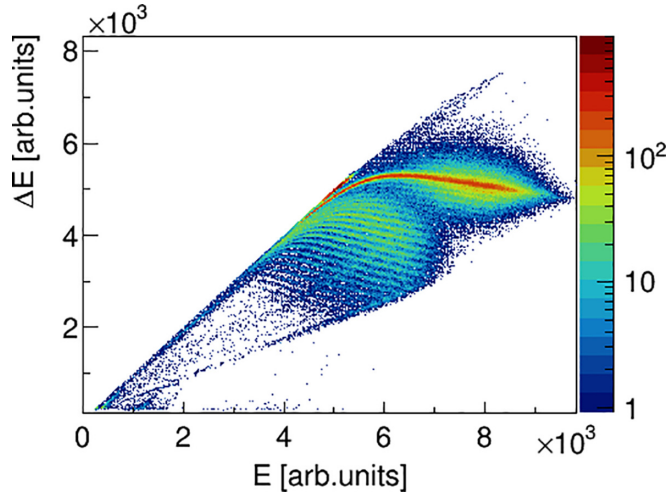

FIG. 1. $\Delta E - E$ matrix obtained for the ^{206}Pb + ^{118}Sn reaction at $E_{\rm lab} = 1200$ MeV, with the spectrometer placed at $\theta_{\rm lab} = 25^\circ$. The most intense band corresponds to the target-like nuclei. Events deriving from fission processes are also visible.

An example of measured $\Delta E - E$ matrix is displayed in Fig. 1. The most intense band corresponds to the target-like ions produced in the multinucleon-transfer process. One also sees fission-like events, which represent only a fraction of their total yield since the spectrometer was set for the detection of transfer products. They could be safely distinguished from the multinucleon transfer events via the time of flight. The visible Z separation indicates the good resolution of the IC. In Fig. 2 a plot of the velocity ($\beta = v/c$) vs in-plane scattering angle ($\theta_{\rm lab}$) is shown together with the calculated Rutherford scattering. The kinematics of the reaction allowed also part of the beam-like ions to enter the spectrometer (lower β), with a distribution bending toward the expected limiting angle for Pb (≈35°), well followed by the calculations. These kinematic constraints helped to monitor the beam energy and the set magnetic field of the spectrometer. From the energy information of the IC we obtained the atomic charge-state (q) distribution, which, combined with the A/q spectra, leads to the final mass distributions. We point out that the large momentum acceptance of the spectrometer ($\Delta p/p = \pm 10\%$) allowed to accommodate most of the atomic charge states with a single setting of the magnetic fields. In Fig. 3 we show, as an example, the mass vs Q-value matrix for Cd ($Z = 48$) isotopes, demonstrating the good mass resolution, $\Delta A/A \approx 1/210$. The crucial procedure to reach such a resolution was the application of the prescription for the optical aberration correction [14,25]. In the trajectory reconstruction, the very

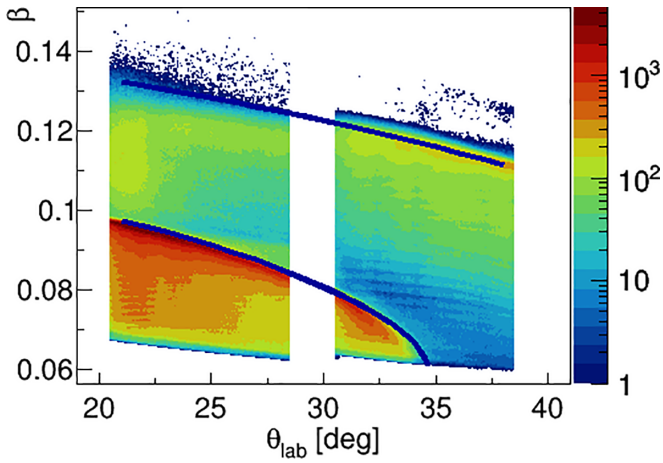

FIG. 2. Matrix of velocity ($\beta = v/c$) vs in-plane scattering angle ($\theta_{\rm lab}$), obtained by merging the measurements performed with the two PRISMA angular and magnetic settings. The events at large and low β correspond to Sn-like and Pb-like ions, respectively. The blue curves correspond to the calculated Rutherford scattering for both fragments.

large longitudinal dimension of PRISMA with respect to the transversal one, as well as the large dimensions of the magnetic elements, ensure that the trajectories are planar after the quadrupole and that the effect of the fringing fields is rather small. Nevertheless, for very heavy ions, the mass resolution can be affected by the presence of optical aberrations due to higher-order magnetic fields which can deviate the ions trajectory from the planarity. Thus, an additional empirical correction has been applied, by polynomial linearization of the A/q bands as a function of the position at the entrance and focal-plane detectors. These corrections are implemented in the mass vs Q-value spectra. In the case of Sn isotopes, due to the overwhelming elastic yield, the atomic charge state resolution was not sufficient to remove the typical A/q repetitive pattern, which generates some degree of overlap for near-by masses. We estimated that the possible overcounting of yields of the ($\pm 2n$) channels is at most ≈20% and

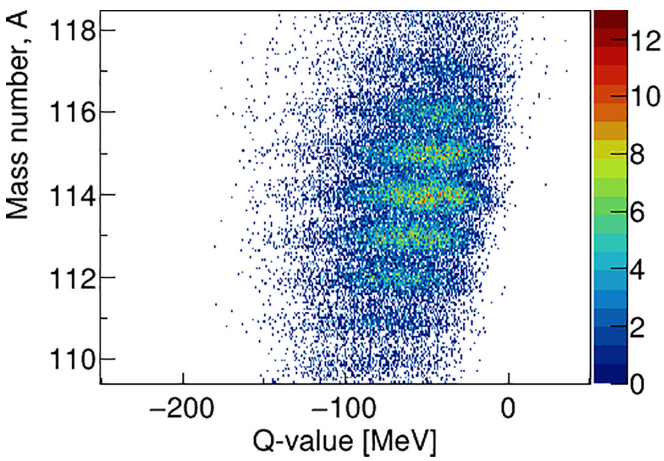

FIG. 3. Mass vs Q-value matrix for Cd isotopes at $\theta_{\rm lab} = 35^\circ$.

larger for the weaker neutron transfer channels, therefore the analysis has been limited to the ($\pm 1n$) and ($\pm 2n$) channels only.

III. ENERGY LOSS DISTRIBUTIONS

The large acceptance of PRISMA gives an excellent opportunity to follow the details of the energy dissipated in the reaction in its evolution from the quasielastic to the deep-inelastic regimes. The most suitable way to represent this evolution is via a two-dimensional matrix of Q value (or alternatively kinetic energy) vs scattering angle, traditionally called Wilczynski plot [26]. We constructed the Wilczynski plots selecting in mass and charge the transfer reaction products. The Q values were generated by assuming a binary reaction and imposing the conservation of momentum. In Fig. 4 we show, as an example, the plot for the ($+1n$) channel together with the projections onto the Q-value axis at selected center of mass angles. One sees that at more forward scattering angles the distribution is dominated by a QE peak, located close to the ground-to-ground state Q value ($Q_{\rm g.s.}$). Such a region becomes progressively unpopulated when moving to angles more backward than the grazing one ($\theta_{\rm c.m.} \simeq 109^\circ$). At the same time, the large energy-loss components become more important and tend to acquire a Gaussian-like shape. We point out that the energy and angular acceptance of the spectrometer [27,28] may alter the final shapes for these very large energy losses, at least to some extent.

The Wilczynski plots and their projections on the Q-value axis around the grazing angle, shown in Figs. 5 and 6, respectively, are displayed for the strongest channels in the vicinity of the entrance-channel mass partition, namely those involving one and two neutrons, and one and two protons. One can follow well the whole event distributions, from the regions close to the $Q_{\rm g.s.}$ to energy losses up to ≈150 MeV. The Wilczynski plots show clearly that the reaction is dominated by the high Coulomb field and one can observe the progressive increase of the large energy-loss components towards backward angles, at variance with the reactions with medium-mass projectiles on heavy targets [7,13,29–35]. We wish to point out that the here presented high resolution data allow to visualize this behavior for energy loss components much smaller (compared to the kinetic energy of elastic events) than the systems previously measured with higher efficiency but lower resolution.

On Fig. 6 one sees that for pure neutron transfers the distributions peak close to the $Q_{\rm g.s.}$, with events extending to larger energy losses. Only in the elastic + inelastic channel the (narrow) quasielastic peak turns out to be well separated from the large energy-loss components. For channels involving proton and neutron stripping the distributions initiate near the optimum Q values (differing by a few MeV from the $Q_{\rm g.s.}$) but peak at large values, indicating that evaporation of neutrons may be expected. One notices that the channels involving a large number of transferred nucleons, like the isotopes belonging to the two proton stripping, have similar Q-value shapes, and for the neutron strippings, reflect the one of the strongest mass. This is what one can expect when these channels receive contributions due to evaporation from nearby

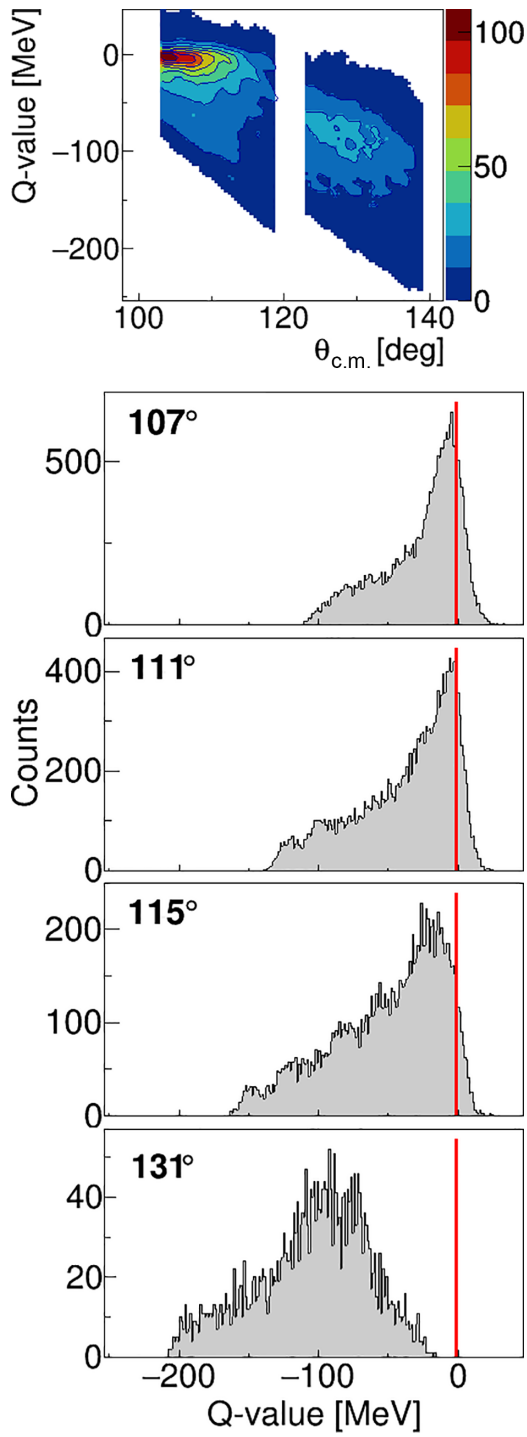

FIG. 4. Matrix of Q value vs center of mass angle $\theta_{\text{c.m.}}$ for the $(+1n)$ channel (top). The matrix is displayed by matching the measured events at the two PRISMA angular and magnetic settings. The panels below show the projections onto the Q-value axis at the indicated center of mass angles (corresponding to $\theta_{\text{lab}} = 36.5^\circ, 34.5^\circ, 32.5^\circ$, and 24.5° starting from the higher spectrum, with $\Delta\theta_{\text{lab}} \simeq 2^\circ$). The vertical (red) lines represent the ground-to-ground state Q value.

higher masses with larger yields. This situation, for the two proton stripping, holds also along the neutron pick-up side. On the other hand, we have to keep in mind that the overall effect of the evaporation on the integrated yields of each neutron pick-up channel is much less significant, since higher mass channels have progressively lower primary cross sections. The one proton transfer channels have a behavior in between the pure neutron transfers and the two-proton stripping chain, in terms of energy losses and effects of evaporation. The details of the shapes may depend on specific nuclear structure or dynamics effects.

IV. CROSS SECTIONS AND COMPARISON WITH THEORY

Differential cross sections have been extracted for the measurement performed with PRISMA at $\theta_{\text{lab}} = 35^\circ$ (near the grazing angle), where the flux for few nucleon-transfer channels has major components close to the quasielastic region. For the elastic + inelastic and pure neutron-transfer channels the cross sections could be extracted also with PRISMA at $\theta_{\text{lab}} = 25^\circ$. At both angular settings the quasielastic part has been obtained by integrating the range from $Q_{\text{g.s.}}$ to ≈ -35 MeV, close to the valley visible in the Q-value spectrum of the $(0n)$ channel. The reliability of the method has been tested by employing different integration procedures, also in the Wilczynski plots. For the channels involving protons, where the deep-inelastic components could not be separated, only an integration of the full Q-value distributions with PRISMA at $\theta_{\text{lab}} = 35^\circ$ has been applied.

The obtained angular distributions for selected channels are shown in Fig. 7, where the filled circles correspond to the integration of the full Q-value range and the empty circles to the integration of the quasi-elastic components only. In the figure are also shown the calculations performed with the GRAZING code [36,37]. The data are plotted in a restricted angular range, i.e., without the edges of the distribution which can be affected by the acceptance of the spectrometer. The quasielastic distributions have been obtained by matching the two PRISMA angular and magnetic settings. The elastic + inelastic data are shown as a ratio to the Rutherford cross sections. The absolute scale of cross sections has been obtained by normalizing the differential angular distribution of the $(+1n)$ channel to the GRAZING computed one (see also Refs. [10,14]). The normalization constant, which has been kept the same for all neutron and proton transfer channels, provides also a consistent description of the elastic + inelastic over Rutherford cross section.

The data have been compared with the GRAZING code, whose main characteristics are briefly reminded below. In GRAZING, two ions interact via a Coulomb plus nuclear interaction and may exchange nucleons. The relative motion of the system is calculated in a nuclear plus Coulomb field. The two nuclei are described as an ensemble of independent nucleons, the basic degrees of freedom being surface vibrations and single particle degrees of freedom. For the excitation of the surface modes the model employs the macroscopic approximation whose form factors are proportional to the r derivative of the ion-ion potential and whose strength are given by the experimental $B(E\lambda)$. The model, for each transfer mode, stripping, and pick-up of neutrons and protons, uses a representative form factor that is parametrized in accordance with [38], taking into account the single-particle properties

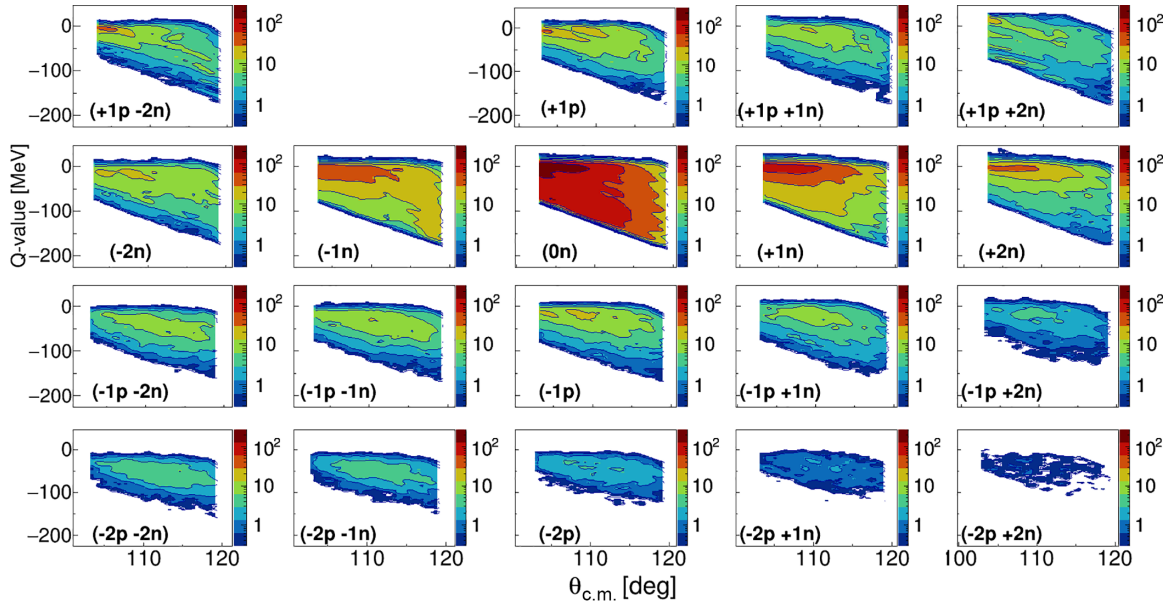

FIG. 5. Wilczynski plots (Q value vs $\theta_{\text{c.m.}}$) measured at $\theta_{\text{lab}} = 35^\circ$ for the labeled transfer channels. The contours represent the double-differential cross sections, $\frac{d^2\sigma}{d\Omega dQ}$. The yield for the $(+1p - 1n)$ channel could not be safely extracted due to partial overlap with the ^{118}Sn one.

of the two colliding ions. The different single-particle states that are participating to the transfer process are described by introducing average single particle level densities. The treatment of the transfer degrees of freedom is based on the assumption that in a heavy-ion collision the exchange of a nucleon may proceed via many open channels that are all quite weak, so that they may be treated as independent modes. Thus, the exchange of nucleons is treated independently and in the successive approximation.

Figure 7 shows that the calculations well describe the elastic + inelastic over Rutherford distribution, in particular the fall-off at angles beyond the quarter point, indicating the correct treatment of the absorption. Calculations also well reproduce the one nucleon-transfer channels, demonstrating the correct treatment of the form factors and the chosen range of partial waves. The fact that a quite good agreement holds also for the channels involving the one-proton stripping and neutron pick-up indicates their direct nature. A similar agreement

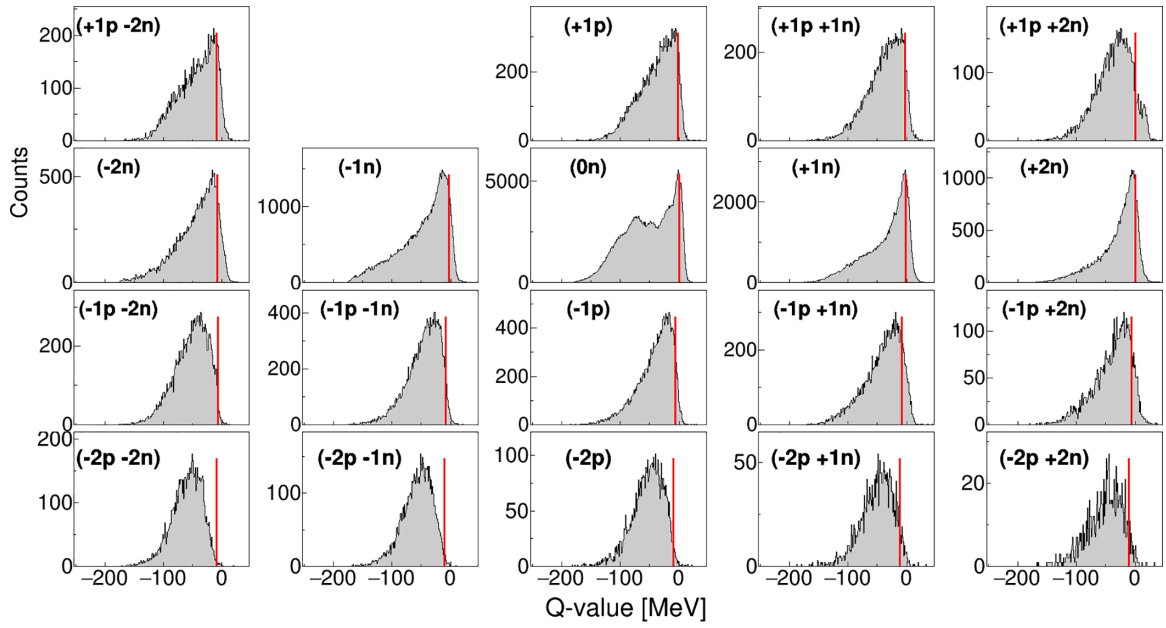

FIG. 6. Q-value distributions measured at $\theta_{\text{lab}} = 35^\circ$ for the labeled transfer channels. The yield for the $(+1p - 1n)$ channel could not be safely extracted due to partial overlap with the ^{118}Sn one. Vertical lines indicate the ground-to-ground state Q values.

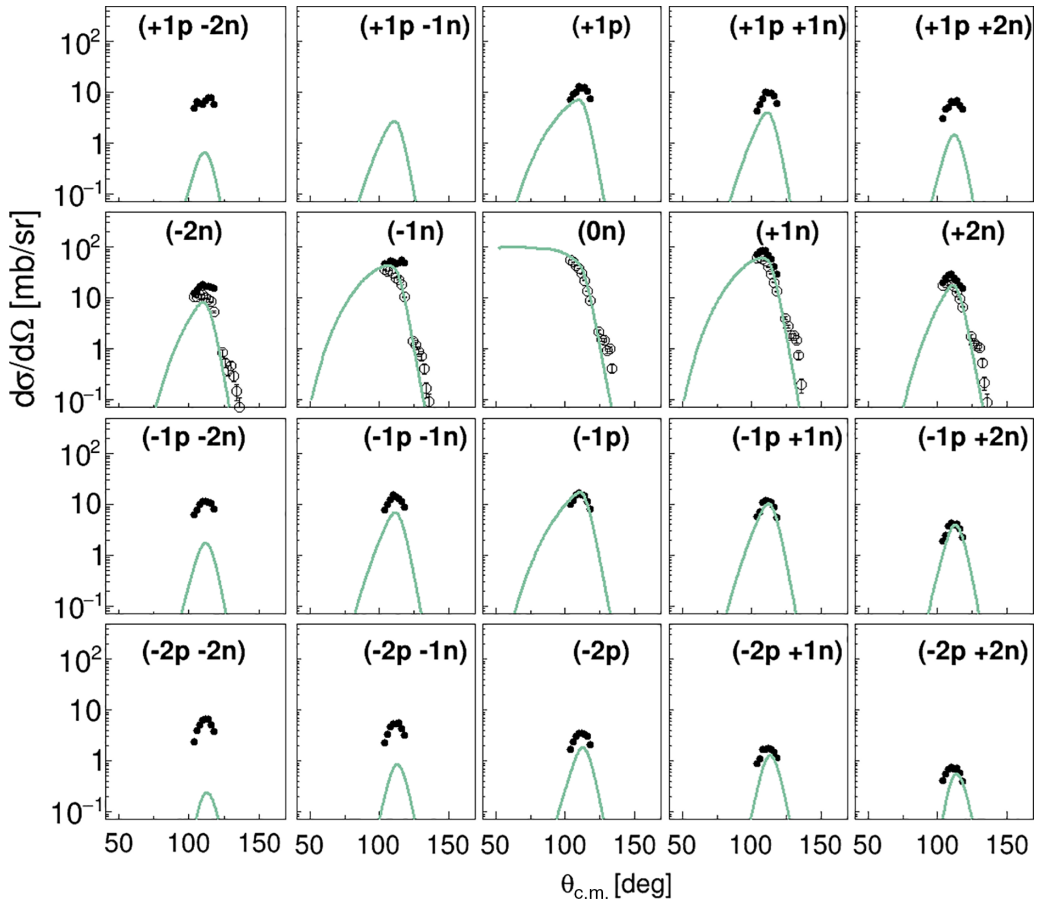

FIG. 7. Experimental differential cross sections (points) compared with GRAZING calculations (lines) without including effects of neutron evaporation. The filled circles correspond to the integration of the full Q values while the empty circles correspond to the quasielastic part only (integration in the range from the $Q_{\text{g.s.}}$ to ≈ -35 MeV). The elastic + inelastic channel is plotted as a ratio over the Rutherford cross section (multiplied by 100). The experimental cross section for the $(+1p-1n)$ channel could not be safely extracted due to partial overlap with the ^{118}Sn yield. Experimental errors are the statistical ones only. The relative normalization between the different PRISMA settings at $\theta_{\text{lab}} = 25^\circ$ and 35° was obtained by using the elastically scattered ^{118}Sn ions in the monitor detector placed at 58°.

for the one-proton-pick-up is not achieved, presumably due to an underestimation of the strength of the form factor. This underestimation propagates for the other channels involving neutron pick-up, though the shapes are always well reproduced. Along the neutron stripping side, more influenced by neutron evaporation, calculations underestimate progressively the absolute values.

The main features just discussed for the angular distributions can be also seen in the total cross sections, shown in Fig. 8 for the wealth of observed transfer channels. The experimental values have been obtained by integrating the differential cross sections assuming a Gaussian shape. One observes how the pure neutron transfer channels are well reproduced by calculations. The same holds for the pure $(-1p)$ channel. Along the proton-stripping side, the experimental cross sections tend to shift toward lower masses and are progressively underestimated by GRAZING. We remind that the primary cross sections for channels involving neutron stripping may be significantly modified by the evaporation of neutrons from the close-by larger masses. This leads to a reshuffling of the final mass distribution, which indeed affects more significantly the lower mass region of the populated isotopes.

The difference between proton and neutron transfers in the comparison of the experimental and calculated cross sections was already noticed in previously studied systems with medium-mass projectiles [7,9,39]. Besides the influence of the larger energy losses for channels involving proton transfers, this was partly attributed to the large modification in the trajectories of entrance and exit channels due to the charge transfer [13], which may not be fully taken into account by theory. The discrepancies with theory for the two proton transfer channels may also indicate the possible presence of additional degrees of freedom (pair-transfer modes), as discussed in the works of Refs. [9,39]. To what extent they play a role is still an issue. More in general, in the case of proton transfer, some prescriptions in theory may need to be revisited, since the single-particle level density and corresponding form factors are less known. An improved understanding is particularly relevant for the proton pick-up channels since they pave the path towards the population of the neutron-rich heavy nuclei.

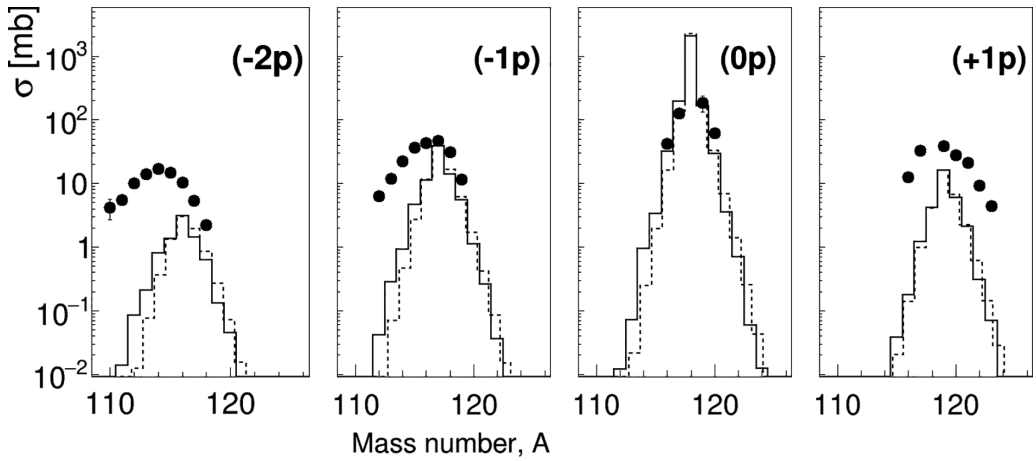

FIG. 8. Experimental (points) and GRAZING calculated (histograms) total angle and Q-value integrated cross sections for the various transfer channels populated in the ^{206}Pb + ^{118}Sn reaction at $E_{lab} = 1200$ MeV. Experimental errors are only statistical ones, and are almost all within the size of symbols. The solid and dashed histograms are the calculations performed with and without evaporation, respectively. The experimental cross sections for the pure neutron transfers have been extracted only for the $(\pm 1n)$ and $(\pm 2n)$ channels and only for the quasielastic part of the Q values (see text for details). Due to the overwhelming elastic yield the cross section for $(+1p - 1n)$, corresponding to ^{118}Sb, is not included.

V. CONCLUSIONS

Multineutron- and multiproton-transfer channels have been successfully measured with high resolution in the ^{206}Pb + ^{118}Sn system at $E_{lab} = 1200$ MeV for nuclei in the $A \approx 120$ mass range, exploiting the performance of the large solid angle magnetic spectrometer PRISMA. By inspecting at the details of the dependence of the Q-value distributions on scattering angle and mass and charge of the transfer products, we could follow the evolution from quasielastic to deep inelastic processes and correlate this evolution to the behavior of the extracted differential and total cross sections. At least for few nucleon transfer channels, these main observables, Q values, and cross sections, retain the main characteristics of direct processes. For the transfer channels involving many nucleons, the large energy loss unavoidably leads to a reshuffling in the final yield distributions.

From the comparison of the experimental cross sections with those calculated with the GRAZING code, an overall good agreement is found for most of few nucleon transfer channels. The quality of agreement demonstrates, also for the case of the presently studied heavy system, the correctness of the used nuclear potential and the chosen range of partial waves that contribute to the cross sections. On the other hand, the progressive underestimation of the yield as more nucleon transfers are involved may indicate that more complicated processes populate the given isotopes, not well taken into account by theory. The observed different behavior between the proton stripping and proton pick-up channels, particularly relevant for the production of neutron rich heavy nuclei, is presently not fully understood. It is important to further pursue studies of the proton transfers and, in particular, to improve their theoretical description.

ACKNOWLEDGMENTS

We acknowledge the whole LNL accelerator group in providing the high-quality ^{206}Pb beam exploiting the highest performance of the PIAVE - ALPI accelerator complex. We acknowledge also the LNL target laboratory for making high-quality targets. This work was partly supported by the ENSAR2 Grant Agreement No. 654002, and by the Croatian Science Foundation Project no. IP-2018-01-1257, and in part by the Center of Excellence for Advanced Materials and Sensing Devices (Grant No. KK.01.1.1.01.0001). M.S. is supported by U.S. Department of Energy, Office of Science, Office of Nuclear Physics, under Contract No. DE-AC02-06CH11357. This work was also partly supported by the National Science Centre, Poland (NCN) (Grant No. 2020/39/D/ST2/00466).

[1] W. von Oertzen and A. Vitturi, Rep. Prog. Phys. **64**, 1247 (2001).
[2] L. Corradi, G. Pollarolo, and S. Szilner, J. Phys. G: Nucl. Part. Phys. **36**, 113101 (2009).
[3] C. H. Dasso, G. Pollarolo, and A. Winther, Phys. Rev. Lett. **73**, 1907 (1994).
[4] D. Montanari, L. Corradi, S. Szilner, G. Pollarolo, E. Fioretto, G. Montagnoli *et al.*, Phys. Rev. Lett. **113**, 052501 (2014).
[5] L. Corradi, S. Szilner, G. Pollarolo, T. Mijatović, D. Montanari, E. Fioretto, A. Goasduff, D. Jelavić Malenica, G. Montagnoli, and A. M. Stefanini, Phys. Lett. B **834**, 137477 (2022).
[6] C. L. Jiang, K. E. Rehm, H. Esbensen, D. J. Blumenthal, B. Crowell, J. Gehring, B. Glagola, J. P. Schiffer, and A. H. Wuosmaa, Phys. Rev. C **57**, 2393 (1998).

[7] L. Corradi, A. M. Stefanini, C. J. Lin, S. Beghini, G. Montagnoli, F. Scarlassara, G. Pollarolo, and A. Winther, Phys. Rev. C **59**, 261 (1999).
[8] L. Corradi *et al.*, Phys. Rev. C **63**, 021601(R) (2001).
[9] S. Szilner *et al.*, Phys. Rev. C **71**, 044610 (2005).
[10] S. Szilner, C. A. Ur, L. Corradi, N. Marginean, G. Pollarolo, A. M. Stefanini *et al.*, Phys. Rev. C **76**, 024604 (2007).
[11] Y. X. Watanabe, Y. H. Kim, S. C. Jeong, Y. Hirayama, N. Imai, H. Ishiyama *et al.*, Phys. Rev. Lett. **115**, 172503 (2015).
[12] A. Vogt *et al.*, Phys. Rev. C **92**, 024619 (2015).
[13] T. Mijatović, S. Szilner, L. Corradi, D. Montanari, G. Pollarolo, E. Fioretto *et al.*, Phys. Rev. C **94**, 064616 (2016).
[14] F. Galtarossa, L. Corradi, S. Szilner, E. Fioretto, G. Pollarolo, T. Mijatović *et al.*, Phys. Rev. C **97**, 054606 (2018).
[15] V. Zagrebaev and W. Greiner, Phys. Rev. Lett. **101**, 122701 (2008).
[16] K. Sekizawa and S. Ayik, Phys. Rev. C **102**, 014620 (2020).
[17] K. Sekizawa, Front. Phys. **7**, 20 (2019).
[18] C. Li, J. Tian, and F. S. Zhang, Phys. Lett. B **809**, 135697 (2020).
[19] C. Simenel and A. Umar, Prog. Part. Nucl. Phys. **103**, 19 (2018).
[20] T. Mijatović, Front. Phys. **10**, 965198 (2022).
[21] D. M. Brink, Phys. Lett. B **40**, 37 (1972).
[22] P. Čolović, S. Szilner, A. Illana, J. J. Valiente-Dobón, L. Corradi, G. Pollarolo *et al.*, Phys. Rev. C **102**, 054609 (2020).
[23] G. Montagnoli *et al.*, Nucl. Instrum. Methods Phys. Res. A **547**, 455 (2005).
[24] S. Beghini *et al.*, Nucl. Instrum. Methods Phys. Res. A **551**, 364 (2005).
[25] F. Galtarossa, Multinucleon transfer in the ^{197}Au + ^{130}Te reaction studied with a high-resolution kinematic coincidence, Ph.D. thesis, University of Ferrara, 2018.
[26] J. Wilczynski, Phys. Lett. B **47**, 484 (1973).
[27] D. Montanari *et al.*, Eur. Phys. J. A **47**, 4 (2011).
[28] T. Mijatović *et al.*, Eur. Phys. J. A **52**, 113 (2016).
[29] A. Gobbi and W. Norenberg, in *Heavy Ion Collisions*, Vol. 2, edited by R. Bock (North-Holland, Amsterdam, 1980).
[30] W. U. Schroder and J. R. Huizenga, Annu. Rev. Nucl. Sci. **27**, 465 (1977).
[31] D. H. E. Gross and H. Kalinowski, Phys. Rep. **45**, 175 (1978).
[32] S. Pontoppidan *et al.*, Phys. Rev. C **28**, 2299 (1983).
[33] W. Mayer, G. Beier, J. Friese, W. Henning, P. Kienle, H. J. Körner, W. A. Mayer, L. Müller, G. Rosner, and W. Wagner, Phys. Lett. B **152**, 162 (1985).
[34] K. E. Rehm, A. M. van den Berg, J. J. Kolata, D. G. Kovar, W. Kutschera, G. Rosner, G. S. F. Stephans, and J. L. Yntema, Phys. Rev. C **37**, 2629 (1988).
[35] R. Płaneta, K. Kwiatkowski, S. H. Zhou, V. E. Viola, H. Breuer, M. A. McMahan, W. Kehoe, and A. C. Mignerey, Phys. Rev. C **41**, 942 (1990).
[36] A. Winther, Nucl. Phys. A **572**, 191 (1994).
[37] A. Winther, Nucl. Phys. A **594**, 203 (1995).
[38] J. M. Quesada, G. Pollarolo, R. A. Broglia, and A. Winther, Nucl. Phys. A **442**, 381 (1985).
[39] L. Corradi *et al.*, Phys. Rev. C **66**, 024606 (2002).